Quantized thermal conductance at low temperatures in quantum wire with catenoidal contacts

Xiao-Fang Peng, Ke-Qiu Chen,* Qing Wan, and B. S. Zou
Key Laboratory for Micro-Nano Optoelectronic Devices of Ministry of Education and Department of Applied Physics, Hunan University, Changsha 410082, China

Wenhui Duan
Department of Physics, Tsinghua University, Beijing 100084, China

(Received 12 February 2010; revised manuscript received 8 April 2010; published 24 May 2010)

The thermal conductance associated with the lowest six types of ballistic phonon modes in quantum wire with catenoidal contacts is investigated. The results show that the cutoff frequency for the four types of acoustic modes is zero while two types of optical modes are of nonzero cutoff frequency. For a perfect quantum wire, a quantized thermal-conductance plateau can be observed. While for the structure with catenoidal contacts, the thermal-conductance plateau is broken and a decrease in thermal conductance appears. The results also show that the reduced thermal conductance contributed from different vibrational modes has different characteristics.

DOI: 10.1103/PhysRevB.81.195317 PACS number(s): 73.63.Rt, 63.22.−m, 62.30.+d, 44.10.+i

I. INTRODUCTION

The thermal transport properties in quantum structures have attracted increasing attention in recent years. Many interesting physical effects are found in these systems such as the universal quantized thermal conductance,[1–3] thermal rectification effects,[4–6] negative differential thermal resistance,[7,8] and so on. Quantized thermal conductance by ballistic phonon at low temperatures have also been predicted theoretically in dielectric quantum wires with catenoidal contacts,[1,9,10] in carbon nanotubes,[11] and by electrons in one-dimensional wire.[12] Quantized thermal conductance by phonons[2] and by photons[13,14] have also been observed experimentally, and the universal thermal quantum is always $\pi^2 k_B^2/3h$. This indicates that the thermal-conductance quantum is independent of the types of energy carriers, as reviewed by Wang *et al.*[15] The thermal-conductance properties have also been reported in various geometries such as quantum waveguides with abrupt junctions,[16] rough surfaces,[17] structural defects,[18] and stub structures,[19,20] nanotubes,[21,22] graphene nanoribbons,[23] and so on. Now, it is known that the lowest six vibrational modes with different characteristics include four types of acoustic modes (namely, the dilatational, torsional, and two types of flexural modes) and two types of optical modes (namely, two shear modes). In spite of all of these advancements, theoretical treatment of the ballistic phonon modes in quantum structures is still under debate. Moreover, most of studies are restricted to thermal conductance of longitudinal (dilatational) mode. The thermal-conductance properties for the other five types of vibrational modes were paid very little attention.

In the present work, we study the thermal conductance contributed from the lowest six lattice vibrational modes in quantum wires with catenoidal contacts, as shown in Fig. 1. The properties of thermal conductance in such structure have also been reported theoretically.[1,10] Rego *et al.* predicted the universal quantum of thermal conductance. However, their numerical studies are limited to only dilatational (longitudinal) mode. Tanaka *et al.*[10] studied the thermal conductance of the six lowest vibrational modes in the same structure. However, in their calculation of transmission rate, a nonzero cutoff frequency appears for the catenoidal structure.[1,10] In the present work, we derive a formula to calculate the acoustic-phonon transport rate for the catenoidal structure, and find that the cutoff frequency for the dilatational mode should be zero, instead of nonzero cutoff frequency.

This paper is organized as follows. Section II presents a detail description of the model and the formulas used in calculations. The numerical results are given in Sec. III with analyses. Finally, a summary is made in Sec. IV.

II. MODEL AND FORMALISM

We model the quantum structure with catenoidal contacts as illustrated in Fig. 1. Two heat reservoirs with temperatures T_1 and T_2 are connected by a catenoidal contacts. It is assumed that the difference $\delta T(\delta T = T_1 - T_2 > 0)$ is very small. So we can adopt the mean temperature T $[T=(T_1+T_2)/2]$ as the temperature of the structure in following calculations. For such a structure, the thermal conductance K for each type of vibrational mode can be expressed as[1]

$$K = \frac{\hbar^2}{k_B T^2} \sum_i \frac{1}{2\pi} \int_{\omega_i}^{\infty} \tau_i(\omega) \frac{\omega^2 e^{\beta\hbar\omega}}{(e^{\beta\hbar\omega}-1)^2} d\omega. \quad (1)$$

Here $\tau_i(\omega)$ is the transmission rate for each vibrational mode through the structure and ω_i is the cutoff frequency of the ith mode. $\beta = 1/(k_B T)$, k_B is the Boltzman constant, T is the temperature, and $\hbar$ is the Plank's constant. The effect of scattering of the catenoidal contacts is introduced through the transmission possibility, $\tau_i(\omega)$, which determines the thermal conductance. The key issue in predicting the thermal conductance is to calculate the transmission possibility, $\tau_i(\omega)$.

For the present structure, the equation of the motion for dilatational mode can be written as[24]

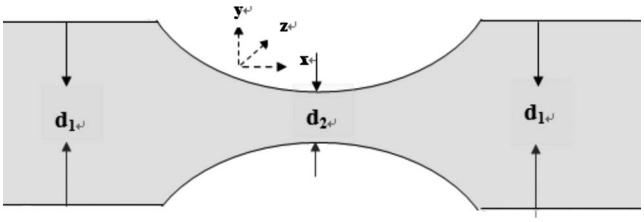

FIG. 1. Two heat reservoirs with temperatures T_1 and T_2 are connected by a catenoidal wire with a rectangular cross-sectional area $A(x)=hl(x)$ [h is thickness in the z direction and $l(x)=\cosh^2(x/\lambda)$].

$$-\sigma(x)A(x)+\left[\sigma(x)+\frac{\partial\sigma(x)}{\partial x}\right]\left[A(x)+\frac{dA(x)}{dx}dx\right]=\rho A(x)dx\frac{\partial^2\Psi}{\partial t^2}, \tag{2}$$

where $A(x)$ is the cross-sectional area $A(x)=A(0)\cosh^2(x/\lambda)=h*L(x)$ and ρ is the mass density. Here, h is a constant and $L(x)=h*\cosh^2(x/\lambda)$ is the width in the y direction. Assuming the material is elastic, the stress of the material can be written as $\sigma=Y\partial\psi/\partial x$. Equation (2) can be simplified as

$$\sigma(x)\frac{\partial A(x)}{\partial x}+\frac{\partial\sigma(x)}{\partial x}A(x)+\frac{\partial A(x)}{\partial x}\frac{\partial\sigma(x)}{\partial x}dx=\rho A(x)\frac{\partial^2\Psi}{\partial t^2}. \tag{3}$$

If ignoring the third item of the left of Eq. (3), then Eq. (3) can be written as

$$\frac{\partial}{\partial x}\left[A(x)Y\frac{\partial\Psi}{\partial x}\right]=\rho A(x)\frac{\partial^2\Psi}{\partial t^2}. \tag{4}$$

According to the expression, it may result in the frequency of acoustic wave satisfying the dispersion relation $\omega^2=v_l^2[k^2+\frac{1}{\lambda^2}]$, as presented in the previous reports.[1,10] This means a cutoff frequency $\omega_D=v_l/\lambda$ will appear for the dilatational mode. This will bring a problem, namely, the cutoff frequency will result in the thermal conductance to be zero, instead of quantized thermal conductance in the limit $T\to 0$. We think that when third item of the left of Eq. (3) is considered, the problem can be solved.

For a nanoscale quantum wire, the stress is related to both the configuration of the structure and the variation in the temperature T so the equation of the motion of the dilatational mode can also be written as

$$-\sigma(x,T)A(x)+\left[\sigma(x,T)+\frac{\partial\sigma_1(x)}{\partial x}dx+\frac{\partial\sigma_2(x)}{\partial x}dx\right]A(x+dx)=\rho A(x+dx)dx\frac{\partial^2\Psi}{\partial t^2}, \tag{5}$$

where $\sigma(x,T)$ is the stress at the position x with temperature T, $A(x+dx)$ is the cross section at the position $x+dx$, and $\frac{\partial\sigma_1(x)}{\partial x}$ is the stress grad derived from the change in the cross section $A(x)$ while $\frac{\partial\sigma_2(x)}{\partial x}$ is induced by change in the temperature along the x direction. Equation (5) can be written as

$$-\sigma(x,T)A(x)+\left[\sigma(x+dx,T)+\frac{\partial\sigma_2(x)}{\partial x}dx\right]A(x+dx)=\rho A(x+dx)dx\frac{\partial^2\Psi}{\partial t^2}. \tag{6}$$

It is well known that, for a quantum wire with temperature T, the thermal equilibrium equation can be written as

$$-\sigma(x,T)A(x)+\sigma(x+dx,T)A(x+dx)=0. \tag{7}$$

From Eqs. (6) and (7), we can get the equation,

$$\frac{\partial\sigma_2(x)}{\partial x}=\rho\frac{\partial^2\Psi}{\partial t^2}. \tag{8}$$

Here, it is presumed that the material behaves elastically and follows the simple Hooke's law,

$$\sigma(x)=Y\frac{\partial\Psi}{\partial x}. \tag{9}$$

The dispersion relation can been written as

$$\omega=v_l k, \tag{10}$$

where, $v_l^2=Y/\rho$ and Y is Young modulus. Obviously, the cutoff frequency is zero regardless of the geometry details. Note that in quantum system, when temperature is low enough, the stress grad due to the change in the temperature and structure may be comparable to the stress itself. So the third item of the left of Eq. (3) cannot be ignored for the present case. However, for the system with large scale and higher temperature, the stress grad originating from the change in the temperature or structure is much smaller than the stress itself, and so the third item of the left of Eq. (3) can be ignored.

For the torsional mode, its equation of motion can be expressed as[25]

$$\rho I(x)\frac{\partial^2\theta}{\partial t^2}=\frac{\partial}{\partial x}\left[C(x)\frac{\partial\theta}{\partial x}\right]. \tag{11}$$

Here, θ is the angle of twist of the wire, $I(x)$ is the polar moment of inertia, and $C(x)$ is the torsional rigidity. For a quantum wire with temperature T, the thermal equilibrium equation for the torsional mode can be written as

$$-M(x,T)+M(x+dx,T)=0, \tag{12}$$

here, $M(x,T)=C(x)\partial\theta/\partial x$ is the torque at the position x with temperature T. Equation (12) can be written as

$$-C(x)\frac{\partial\theta(x,T)}{\partial x}+C(x+dx)\frac{\partial[\theta(x+dx,T)]}{\partial x}=0. \tag{13}$$

Equation (13) can be further written as

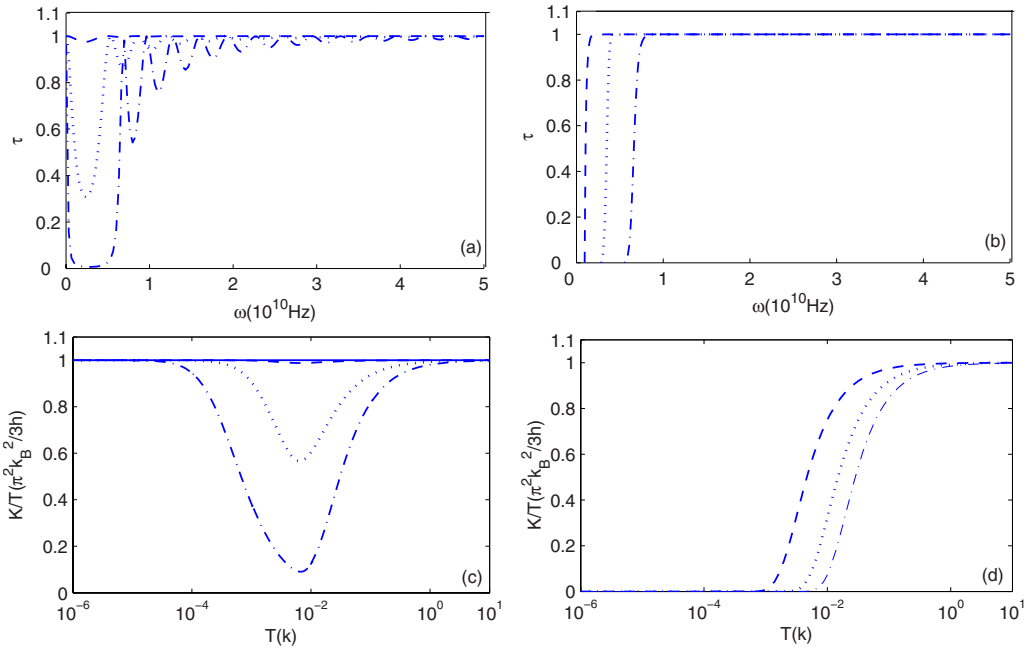

FIG. 2. (Color online) (a) and (b) describe the transmission rate versus reduced frequency $\omega h/v_l$ of the dilatational mode with the third item of the left of Eq. (1) being considered and ignored, respectively. The dashed, dotted, and dashed-dotted curves correspond to $d_1=2000$, $d_2=50$, $\lambda=860$, and $h=50$ nm; $d_1=200$, $d_2=50$, $\lambda=86$, and $h=50$ nm; and $d_1=20$, $d_2=10$, $\lambda=86$, and $h=10$ nm. (c) and (d) describe the corresponding thermal conductance divided by temperature K/T reduced by the zero-temperature universal value $\pi^2k_B^2/3h$ for (a) and (b), respectively. All structural parameters are same as (a) and (b). The solid curve in (c) is the reduced thermal conductance for an ideal quantum wire with structural parameters $d_1=d_2=2000$ nm.

$$-C(x)\frac{\partial\theta(x,T)}{\partial x}+C(x+dx)\frac{\partial\left[\theta(x,T)+\frac{\partial\theta_1(x)}{\partial x}dx\right]}{\partial x}=0, \tag{14}$$

where $\frac{\partial\theta_1(x)}{\partial x}$ is the angle grad derived from the change in the cross section $A(x)$. The equation of motion of the torsional mode can be written as

$$-C(x)\frac{\partial\theta(x,T)}{\partial x}+C(x+dx)\frac{\partial\left[\theta(x,T)+\frac{\partial\theta_1(x)}{\partial x}dx+\frac{\partial\theta_2(x)}{\partial x}dx\right]}{\partial x}=\rho I dx\frac{\partial^2\theta}{\partial t^2}, \tag{15}$$

here, $\frac{\partial\theta_2(x)}{\partial x}$ is induced by change in the temperature along the x direction. From Eqs. (14) and (15), we can get the equation,

$$C(x+dx)\frac{\partial^2\theta(x)}{\partial x^2}=\rho I\frac{\partial^2\theta}{\partial t^2}. \tag{16}$$

From Eq. (16), we can derive the dispersive relation of the torsional mode,

$$\omega=\frac{C}{\rho I}k. \tag{17}$$

From Eq. (17), it is known that the cutoff frequency of the torsional mode is zero and the torsional mode is also acoustic mode.

In our calculations, the equations of motion for the two flexural modes and two shear modes are same as the equations given in the Ref. 10. Note that the flexural mode is acoustic mode with zero cutoff frequency but the shear mode is optical mode with nonzero cutoff frequency.

Note that in order to numerically calculate the transmission rate for each vibrational mode through the catenoidal wire, we first subdivide the wire into many small segments in the longitudinal x direction so that each segment can be regarded as a uniform cross-sectional area. By using the ballistic boundary conditions and the scattering matrix method,[26] we can calculate the transmission rate and then the thermal conductance can be obtained from Eq. (1). In the follows, we will numerically study the transmission rate and thermal conductance for the lowest six types of vibrational modes. The material for the structure is chosen to be GaAs with $Y=12(10^{10}$ N m$^{-2})$ and $\rho=5317.6$ (kg m^{-3}).[10]

III. NUMERICAL RESULTS AND DISCUSSION

In Figs. 2(a) and 2(c), we describe the transmission rate and thermal conductance for the lowest dilatational mode through the catenoidal structure. As a comparison, in Figs. 2(b) and 2(d), we also give the transmission rate and thermal

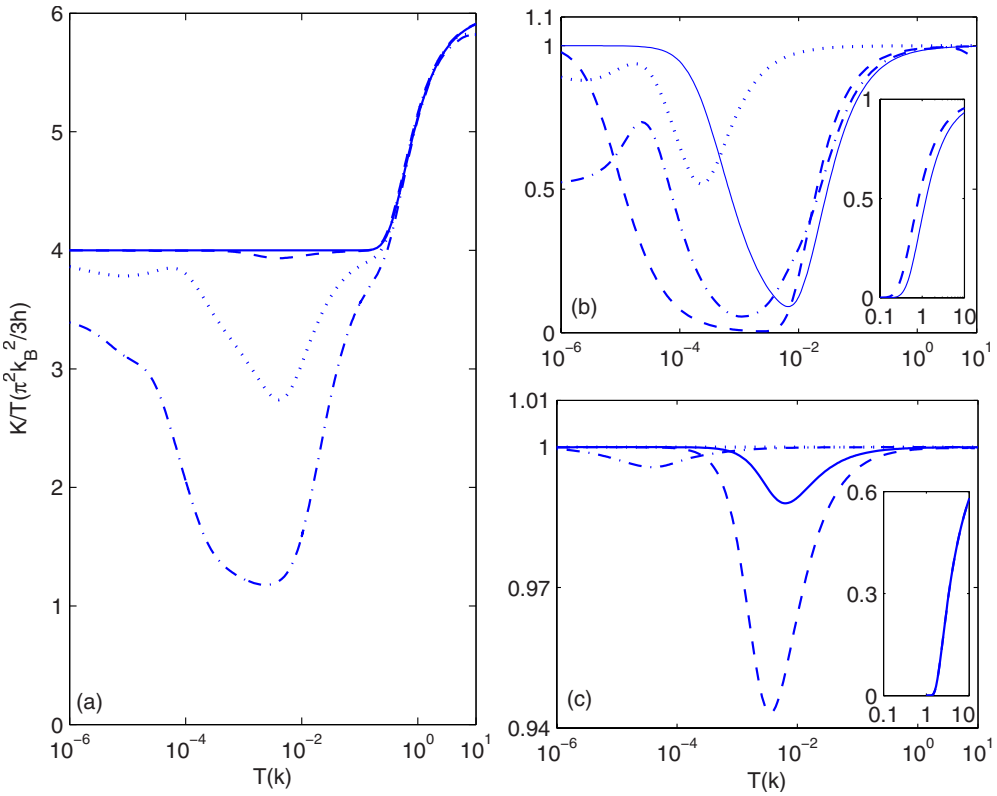

FIG. 3. (Color online) (a) corresponds to the total thermal conductance divided by temperature K/T reduced by the zero-temperature universal value $\pi^2 k_B^2/3h$. The solid, dashed, dotted, and dashed-dotted curves correspond to $d_1=d_2=50$ nm; $d_1=60$, $\lambda=5021.6$ nm; $d_1=200$, $\lambda=1653$ nm; and $d_1=2000$, $\lambda=860$ nm, respectively. Here, we take $d_2=50$, $a=2176.9$, and $h=50$ nm. (b) and (c) correspond to the thermal conductance for the lowest six types of vibrational modes divided by temperature K/T reduced by the zero-temperature universal value $\pi^2 k_B^2/3h$. The solid, dashed, dotted, and dashed-dotted in (b) and (c) correspond to four acoustic modes, namely, dilatational mode, torsional mode, and two flexural modes in z and y direction, respectively. The solid and dashed curves in inserted figure in (b) and (c) correspond to two shear modes in z and y directions, respectively. The structure parameters in (b) and (c) are $d_1=2000$, $\lambda=860$ nm; $d_1=60$, $\lambda=5021.6$ nm, respectively. Here, $d_2=50$, $a=2176.9$, and $h=50$ nm.

conductance when the third item of the left of Eq. (3) is ignored. From Figs. 2(a) and 2(b), it can be found that the transmission spectra display different characteristics in both cases. When this item is ignored, the transport is broken when the frequency is smaller than the cutoff frequency, and the cutoff frequency is dependent on the structural parameters. However, when this item is considered, the transport always exists for all frequencies. The variation in the structural parameters brings different transport characteristics as seen in Fig. 2(a). A wide dip appears in the structure with large difference between d_1 and d_2, and the dip becomes narrow when d_1 gradually approaches d_2, which results from the scattering degree of the structure on phonon being weakened when the difference between d_1 and d_2 is reduced. From Figs. 2(c) and 2(d), it can be found that the thermal conductance also presents different behaviors in both cases the third item of the left of Eq. (3) being considered and ignored. For the former, the reduced thermal conductance always presents a quantum plateau with the value $\pi^2 k_B^2 T/3h$ for perfect quantum wire, which is in agreement with the previous studies.[1,20] While the structure is catenoidal wire, the reduced thermal conductance displays a large dip at certain low-temperature region when $d_1=2000$ nm, and the dip becomes more smaller when d_1 approaches d_2. This can be understood from the transmission dip in Fig. 2(a). The decrease in the thermal conductance results from the attached scattering of the catenoidal structure, and the scattering degree becomes small when d_1 is closed to d_2. However, when $T\to 0$, the reduced thermal conductance is always kept to be the universal value $\pi^2 k_B^2 T/3h$ regardless of the geometry details. These results are also in agreement with the experimental results qualitatively.[2] When the third item of the left of Eq. (3) being ignored, however, the reduced thermal conductance presents fully different behaviors. The reduced thermal conductance arises only when the temperature is higher than the certain temperature where the phonon frequency is higher than the cutoff frequency and is always increased monotonically with increasing temperature. In such case, we cannot observe the thermal-conductance quantum plateau even in perfect quantum wire. This is obviously in disagreement with theoretical[1] and experimental[2] results. This indicates that the third item of the left of Eq. (3) should be considered in calculating thermal conductance.

In Fig. 3(a), we describe the total reduced thermal conductance contributed by the four acoustic modes and two optical modes. When the structure is a perfect quantum wire, a quantized thermal-conductance plateau appears with four units of the universal value $\pi^2 k_B^2 T/3h$ contributed by the four

lowest acoustic modes. With the increase in the temperature, two optical modes also make contribution to the thermal conductance, then the plateau starts to develop at six units of the universal value $\pi^2 k_B^2 T/3h$. However, when the perfect quantum wire is broken and becomes a catenoidal structure, the quantized thermal-conductance plateau is broken, instead a decrease in the thermal conductance appears as the temperature goes up and the degree of decrease is increased when the difference between d_1 and d_2 is increased. This agrees with the experimental result qualitatively.[2] It should be noted that at more lower temperatures, a approximate quantized thermal-conductance plateau can still be observed. Of course, the length of the plateau is shorted. To further understand the reduced thermal-conductance behaviors, in Figs. 3(b) and 3(c), we give the reduced thermal conductance for single vibrational modes. It can be found that the reduced thermal conductances contributed from different vibrational modes have different characteristics. Comparing Fig. 3(b) with Fig. 3(c), we can find that the reduced thermal conductance of single mode is sensitive to the variation in the structural parameters. Though at the case $d_1=2000$ nm, quantized thermal-conductance plateau cannot be observed except the dilatational mode. However, at the case $d_1=60$ nm, quantized thermal-conductance plateau of single acoustic modes at very low temperature can still be observed. From the insets in Figs. 3(b) and 3(c), it can be seen that the reduced thermal conductances of the two optical modes are of similar characteristics but different from those of single acoustic modes. The reduced thermal conductances for both optical modes have cutoff temperature and display monotonic behavior with the variation in the temperature. When d_1 approaches d_2, the reduced thermal conductances of the two optical modes are joined together and are difficult to be distinguished. From these results, it is known that we can observe quantized thermal-conductance plateau with only four units of the value $\pi^2 k_B^2/3h$. This is in agreement with the theoretical predicts for the thermal conductance of single vibrational modes in various kinds of quantum systems such as dielectric quantum wires.[18,19]

IV. SUMMARY

In summary, we study the reduced thermal conductance contributed from the lowest six types of vibrational modes in quantum wire with catenoidal contacts. The results show that the cutoff frequency for the four acoustic modes is zero while the two optical modes are of nonzero cutoff frequency. When the structure is a perfect quantum wire, a quantized thermal-conductance plateau with $4\pi^2 k_B^2/3h$ contributed by the four acoustic modes can be observed. While the structure is a catenoidal structure, the reduced thermal-conductance plateau is broken and a decrease in thermal conductance appears due to the presence of the attached scattering by the catenoidal contact. The reduced thermal conductances for the two optical modes display a monotonic behavior with the variation in the temperature. From these results, it is known that the reduced thermal conductances contributed from different vibrational modes have different characteristics.

ACKNOWLEDGMENTS

This work was supported by the National Natural Science Foundation of China (Grants No. 10674044 and No. 90606001), by the Ministry of Science and Technology of China (Grant No. 2006CB605105), and by the Specialized Research Fund (Grant No. 200805320011).

*Author to whom correspondence should be addressed; keqiuchen@hnu.cn

[1] L. G. C. Rego and G. Kirczenow, Phys. Rev. Lett. **81**, 232 (1998).
[2] K. Schwab, E. A. Henriksen, J. M. Worlock, and M. L. Roukes, Nature (London) **404**, 974 (2000).
[3] T. Yamamoto and K. Watanabe, Phys. Rev. Lett. **96**, 255503 (2006).
[4] B. W. Li, L. Wang, and G. Casati, Phys. Rev. Lett. **93**, 184301 (2004).
[5] C. W. Chang, D. Okawa, A. Majumdar, and A. Zettl, Science **314**, 1121 (2006).
[6] N. Yang, G. Zhang, and B. Li, Appl. Phys. Lett. **95**, 033107 (2009).
[7] B. W. Li, L. Wang, and G. Casati, Appl. Phys. Lett. **88**, 143501 (2006).
[8] W.-R. Zhong, P. Yang, B.-Q. Ai, Z.-G. Shao, and B. Hu, Phys. Rev. E **79**, 050103(R) (2009).
[9] M. P. Blencowe, Phys. Rev. B **59**, 4992 (1999).
[10] Y. Tanaka, F. Yoshida, and S. Tamura, Phys. Rev. B **71**, 205308 (2005).
[11] T. Yamamoto, S. Watanabe, and K. Watanabe, Phys. Rev. Lett. **92**, 075502 (2004).
[12] O. Chiatti, J. T. Nicholls, Y. Y. Proskuryakov, N. Lumpkin, I. Farrer, and D. A. Ritchie, Phys. Rev. Lett. **97**, 056601 (2006).
[13] M. Meschke, W. Guichard, and J. Pekola, Nature (London) **444**, 187 (2006).
[14] T. Ojanen and T. T. Heikkila, Phys. Rev. B **76**, 073414 (2007).
[15] J. S. Wang, J. Wang, and J. T. Lu, Eur. Phys. J. B **62**, 381 (2008).
[16] M. C. Cross and R. Lifshitz, Phys. Rev. B **64**, 085324 (2001).
[17] D. H. Santamore and M. C. Cross, Phys. Rev. Lett. **87**, 115502 (2001).
[18] K.-Q. Chen, W.-X. Li, W. Duan, Z. Shuai, and B.-L. Gu, Phys. Rev. B **72**, 045422 (2005).
[19] P. Yang, Q.-f. Sun, H. Guo, and B. Hu, Phys. Rev. B **75**, 235319 (2007).
[20] X.-F. Peng, K.-Q, Chen, B. S. Zou, and Y. Zhang, Appl. Phys. Lett. **90**, 193502 (2007).
[21] P. Kim, L. Shi, A. Majumdar, and P. L. McEuen, Phys. Rev. Lett. **87**, 215502 (2001).
[22] N. Mingo, D. A. Stewart, D. A. Broido, and D. Srivastava, Phys. Rev. B **77**, 033418 (2008).

[23] Y. Xu, X. Chen, B. L. Gu, and W. Duan, Appl. Phys. Lett. **95**, 233116 (2009).
[24] K. F. Graff, *Wave Motion in Elastic Solids* (Dover, New York, 1975), pp. 108–109.
[25] K. F. Graff, *Wave Motion in Elastic Solids* (Dover, New York, 1975), pp. 126–127.
[26] Wen-Xia Li, Ke-Qiu Chen, Wenhui Duan, Jian Wu, and Bing-Lin Gu, J. Phys. D **36**, 3027 (2003).